

The effect of reaction temperature on the formation of 2H-SiC and 3C-SiC nanowhiskers

Hazlina Dzulkifli^a, Mazli Mustapha^{a*}, Nabihah Sallih^a, Saeid Kakooei^a and Faizal Mustapha^b

^aMechanical Engineering Department, Universiti Teknologi PETRONAS (UTP), 32610 Seri Iskandar, Perak Malaysia

^bDepartment of Aerospace Engineering, Universiti Putra Malaysia, 43400 UPM Serdang, Selangor Darul Ehsan, Malaysia

ARTICLE INFO

Article history:

Received 28 September 2019

Accepted 27 January 2020

Available online

27 January 2020

Keywords:

Silicon carbide

Carbothermal reduction

process

2H and 3C-SiC nanowhiskers

ABSTRACT

Synthesis of 2H and 3C-polytype silicon carbide nanowhiskers mixture of silicon dioxide and carbon was performed by carbothermal reduction process. The reaction temperature for synthesis of 2H-SiC was varied from 1350 °C to 1650 °C and for the 3C-SiC this range was varied from 1450 °C to 1650 °C. Scanning Electron Microscopy (SEM) analyses showed that nanowhiskers structures of both 2H-SiC and 3C-SiC polytypes has a size up to 100 nm in diameters and several microns in length. However, the orientation and pattern of grains were different in both structures. While for 3C-SiC polytype, the shape has been classified as SiC majorly grew along [101] plane by X-ray Diffraction pattern and finalized by Raman shift peaks at 799 and 959 cm⁻¹, the shape of 2H-polytype silicon carbide was categorized as SiC majorly grown along [111] plane confirmed by Raman shift peak at 799 and 963 cm⁻¹. The mechanism of vapor-gas interaction was also suggested and discussed for both SiC nanowhiskers polytypes.

© 2020 Growing Science Ltd. All rights reserved.

1. Introduction

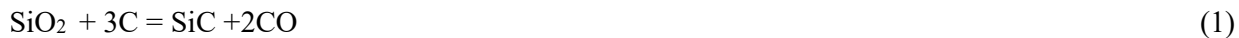
Silicon carbide (SiC) is a chemical compound of carbon and silicon made by a high temperature electro-chemical reaction of sand and carbon and is known as a high quality technical grade ceramic with very good mechanical properties and has unique properties in different areas including (optical and electrical aspects, high corrosion and oxidation resistance, high temperature stability, excellent thermal conductivity, high hardness and strength, wear resistance). These special properties and characteristics have made SiC widely applied in industrial and engineering fields such as aeronautic, cutting tool, semiconductor, electronic components, resistance heating, flame igniters, abrasives, refractories, and numerous high-performance applications (Heidarzadeh et al., 2014; Shi et al., 2006; Petrovic et al., 1985; Xu et al., 1992). More than 200 polytypes of SiC were reported and major polytypes of SiC classified as hexagonal polytypes (α -SiC) and cubical polytypes (β -SiC) respectively (Ito et al. 2014). The most common polytype occurred for α -SiC is 2H-, 4H- and 6H-SiC. Meanwhile, 3C-silicon carbide owned zinc blende structure (i.e. cubic structure) structure with ...ABCABC... sequence is the most synthesized polytype in β -SiC regime (Zhu et al. 2013). The hexagonal have the stacking sequence of ...ABAB... for 2H, ...ABCABC... for 4H, and ...ABCACBABCACB... for 6H. The 2H-SiC possessed the largest band gap among them compared to other polytypes like 3C-, 4H-, and 6H-SiC (Yao

* Corresponding author.

E-mail addresses: mazli.mustapha@utp.edu.my (M. Mustapha)

et al. 2003). The simulation prediction performed by Monte Carlo has been demonstrated higher electron mobility in 2H-SiC than other polytypes (Bertilsson et al., 2001). The electronic structures of these polytypes are rather different and different polytypes have widely ranging physical properties. SiC is a semiconducting material with wide band gap at room temperature, which exhibits excellent electronic properties including high electron mobility and saturated electron drift velocity (Ryn et al., 2001; Pawelec et al., 2002). For example, 3C-SiC has the highest electron mobility and saturation velocity because of reduced phonon scattering resulting from the higher symmetry. The band gaps differ widely among the polytypes ranging from 2.36 eV for 3C-SiC to 3.05 eV in 6H SiC to 3.3 eV for 2H-SiC. In general, the greater the wurtzite component, the larger the band gap. Among the SiC polytypes, 6H is most easily prepared and best studied, while the 3C and 4H polytypes are attracting more attention for their superior electronic properties. The polytypism of the SiC makes it nontrivial to grow single-phase material, but it also offers some potential advantages - if crystal growth methods can be developed sufficiently then heterojunctions of different SiC polytypes can be prepared and applied in electronic devices (Morkoc et al., 1994). Although, there were many reports on the synthesis of the 3C-SiC, 4H-SiC and 6H-SiC polytypes, relatively few dealt with the synthesis of 2H-SiC (Kang et al., 2011; Wu et al., 2015). This is because the free energy between different polytypes is so small that the 2H-SiC is easily transformed to other polytypes of SiC and thus difficult to form (Li et al., 2013). It was also reported that the synthesis of SiC nanowires and nanowhiskers produced the 3C-SiC polytype structure (cubic phase or β -phase) with multiple stacking faults.

There are many methods devoted for synthesizing SiC including sol-gel method (Omidi et al. 2015), microwave heating (Kuang et al., 2013), chemical vapor deposition (Ganiyu et al., 2014), thermal plasma (Moskovskikh et al., 2015) and laser ablation (Lee et al., 2000). The complicated equipment, lengthy period and cost consuming for these methods has limited the usage application for growing of SiC. Therefore, the established conventional and simpler technique well known as carbothermal reduction became the most popular method. Carbothermal reduction or Acheson process involves long hours heating of raw materials at extremely high temperatures which about 2200 - 3300 °C. Quartz sand and petroleum coke are used as precursor material for this technique (Cetinkaya & Eroglu, 2011). Large particles powder are produced because of high temperature and long heating hours. Therefore, the extensive mechanically milling of raw materials are needed to produce smaller diameter size and will aid the reaction to reduce sintering temperature (Moshtaghioun et al., 2011). In thermodynamically aspects, the overall reaction for Acheson process is usually represented by:



This process was involved endothermic reaction with $\Delta H^\circ_{298} = 618.5$ kJ. The grown temperature of SiC initiated at 1500 °C. Temperature above 1600 °C is believed to be gas-gas reaction that yield whiskers formation and the powdery form is produced when temperature is ranging from 1500 to 1600 °C favouring gas-solid reaction. Due to noticeable influence of temperature during the process of SiC formation, in this paper, the effect of temperature on the formation of nanowhiskers 2H-SiC and 3C-SiC by the reaction of silicon dioxide, SiO_2 with carbon is investigated.

2. Experimental procedure

For 3C-SiC formation, the milling machine used was a planetary ball milling with four stations. The amorphous silicon dioxide (SiO_2) with purity of 99.6% was used as a sign material. The mill balls with 5 cm diameters and the SiO_2 inside the mixing tanks of 15 mL are impacted strongly upon high speed movement that was set to 200 RPM, and material was eventually ground into powder to 20:1 ball to powder ratio. The pure powder carbon from petroleum coke and the milled SiO_2 with molar ratio 6:1 were then mixed together beyond the stoichiometric ratio in Eq. (1) in a rotary mixture. The mixture was then put to undergo carbothermal reduction process which leads to modified tube furnace of 250 cm³ heated from ranging 1450 °C up to 1650 °C with 100 °C in sequence (i.e. 1450 °C, 1550 °C and 1650

$^{\circ}\text{C}$). Before that, it was placed inside the ceramic plate with about 2mm powdery bed on top layer of the plate. During 3 hours in time, allotment of sintering process and purging, 15 minutes prior to heating, 100% argon gas was fed into horizontal tube furnace. Once the sintering process had taken place, hydrofluoric acid was used to filter the unreacted SiO_2 and any excess carbon was cleaned by heating 1000 $^{\circ}\text{C}$ in air. Similarly for the formation of 2H-SiC structure, Silicon dioxide, SiO_2 obtained from rice husk was used as precursor material with purity of 99%. The silicon dioxide was ball-milled to 100 hours inside the planetary ball milling with 4 stations. Hardened iron balls (15 cm diameter) was used as milling media and stainless steel jar (15 mL) as a mixing chamber. The grinding speed was set to 200 RPM and ball to powder ratio (BPR) was set to 20:1. Carbon black powder originally from petroleum coke was obtained from PETRONAS refinery. The mechanical milled silicon dioxide and carbon were mixed and placed in a rotary mixture with 6:1 molar ratio beyond the stoichiometric ratio in the Eq. (1). The mixture was then placed inside the ceramic boat with 1-2 mm powdery bed and introduced to modified tube furnace to undergo carbothermal reduction process. The 100% argon gas was fed during sintering process and purging was made into tube furnace 15 minutes prior to heating. The furnace was heated to 1350 $^{\circ}\text{C}$ to 1650 $^{\circ}\text{C}$ with elevation 100 $^{\circ}\text{C}$ for each step. Three hours duration clocked as holding sintering time. After sintering process, the unreacted silicon dioxide was filtered using hydrofluoric acid, HF and excess carbon was cleaned by heating 1000 $^{\circ}\text{C}$ in air.

After production of both 2H and 3C-SiC, Scanning Electron Spectroscopy (SEM) and Energy Dispersive Spectroscopy (EDS) (VPFESEM, Zeiss Supra55 VP) were used to analyze the morphology of the final product. The phase composition was determined by X-ray Diffraction method (XRD) (X' Pert³ Powder & Empyrean, PANalytical) and Raman Spectrometer (Horiba JobinYvon HR800). High Score+ PANalytical software was used to find the XRD Phase identification of the powders.

3. Results and Discussion

Fig. 1 shows general images of Field emission scanning electron microscopy (FESEM) of synthesized 2H-SiC nanostructure. It can be seen clearly that morphology of SiC nanostructure formed at temperature about 1450 $^{\circ}\text{C}$ and continued growing when the temperature is increasing.

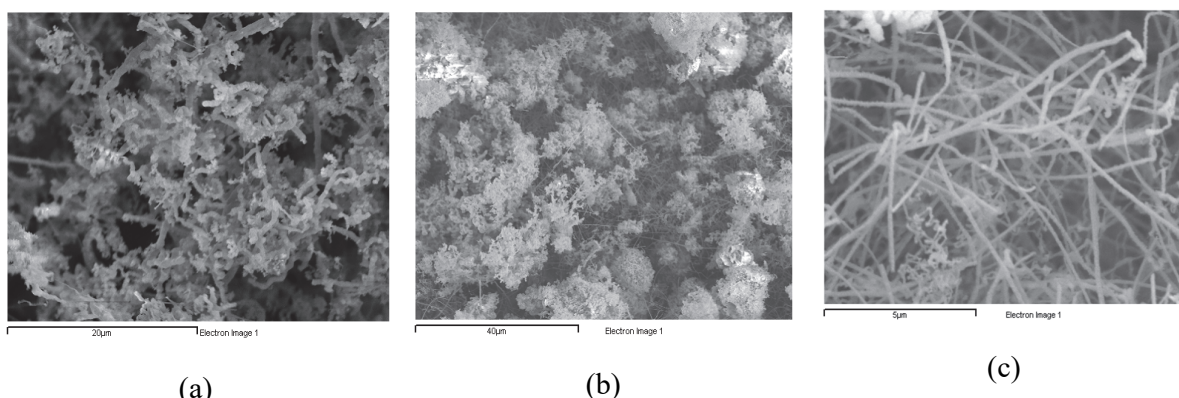


Fig. 1. FESEM images of the 2H-SiC nanowhiskers with different reaction temperatures of (a) 1450 $^{\circ}\text{C}$, (b) 1550 $^{\circ}\text{C}$ and (c) 1650 $^{\circ}\text{C}$

The 2H-SiC with fibrous structure was classified as whiskers type formation. SiC nanowhiskers grown in the random disorder and possessed irregular diameter up to 100 nm with several hundred microns in length. Magnified image in Fig. 1c (with magnification of 5 micro-meter) shows non-smooth surfaces along the nanowhiskers. The EDS analysis of grown nanowhiskers revealed mainly major contain of C and Si product was found. Therefore, it is strongly believed that 2H-SiC nanowhiskers was formed. Similarly, Fig. 2 shows the FESEM images of the 3C-SiC nanowhiskers with different reaction

temperature. In Fig. 2a at temperature of 1450 °C the morphology of 3C-SiC nanostructure was formed visibly. As the temperature is increasingly being at 1550 °C (Fig. 2b), the morphology of 3C-SiC nanostructure continued growing. The 3C-SiC structured with gristly structure was classified as whiskers type formation. SiC nanowhiskers grown in the random disorder and possessed irregular diameter up to 100 nm with several hundred microns in length. Fig. 2c at temperature of 1650 °C shows un-even surfaces along the 3C-SiC nanowhiskers. The growth of nanowhiskers discovered that the whiskers mainly contained major of C and Si elements.

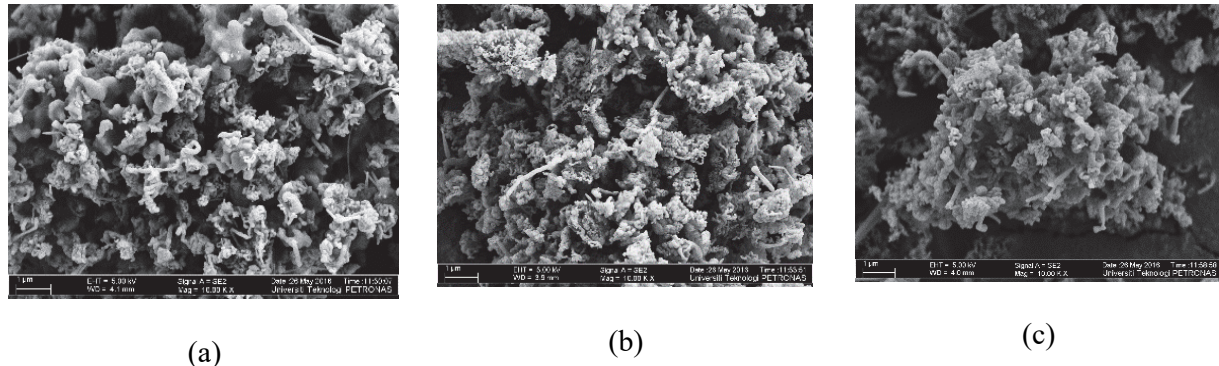


Fig. 2. FESEM images of the 3C-SiC nanowhiskers with different reaction temperature (a) 1450 °C (b) 1550 °C and (c) 1650 °C.

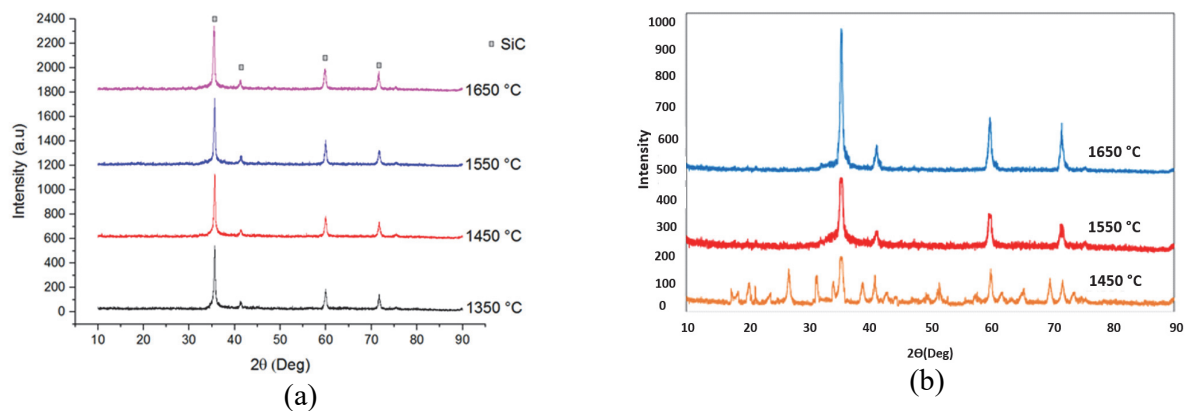


Fig. 3. X-ray diffraction pattern of the (a) 2H-SiC and (b) 3C-SiC products with different heating temperatures

XRD analyses were also performed on each of the 2H-SiC and 3C-SiC samples to determine their phase composition as shown in Fig. 3. For 2H-SiC formation, four diffraction peaks exhibited in XRD pattern at [111], [110], [200] and [220] planes (Fig. 3a). The XRD peaks shows hexagonal configuration of crystal system or α -SiC with close match with standard value (ICSD Reference code: 01-072-4564). The narrow width and distinct peaks of XRD pattern shows that well-formed of 2H-SiC crystalline with the highest intensity peaks at [111] compared to the other three peaks of SiC. This can be inferred that a nanowhisker 2H-SiC was majorly developed at [111] direction. Fig. 3b shows the phase composition of each of these reactions for 3C-SiC obtained by XRD analysis. From the pattern it was clearly seen lots of diffraction peaks ranging between 20 to 80 theta degrees especially at temperature of 1450 °C. The diffraction peaks became lesser and strong as the temperature increased. One strong peak at a range of 30 to 40 theta degrees occurred when temperature reached at 1650 °C. The peaks show hexagonal configuration of crystal system or α -SiC with almost identical with the standard value (JCPDS ICDD: 29-1126). The slim cross-section and the different peaks of XRD pattern show that the 3C-SiC crystalline was well-formed with the highest intensity peak at (101) plane. This can be concluded that a nanowhisker

3C-SiC was mainly developed at (101) direction. This XRD results was later proved by Raman spectroscopy in details.

Raman scattering arises from molecular vibration causing a change in polarizability. This means that intense Raman scattering occurs from symmetric vibrations which induce a large distortion of the electron cloud around the molecule. A peak appearing in the Raman spectrum will be derived from a specific molecular vibration or lattice vibration. Peak position shows the specific vibrational mode of each molecular functional group included in the material. The same vibrational modes for each functional group will show a shift in peak position due to the nearby environment surrounding the functional group, thus it is said the Raman spectrum. Raman spectroscopy was also performed to characterize the as-obtained synthesis products. The typical of SiC spectrum in Raman spectroscopy is shown in Fig. 4. Generally, the bulk 2H-SiC recorded the peaks at 264, 764, 799 and 963 cm⁻¹ as reported relative to literature (Zhang et al. 2010). This pattern indicated a significant peak around 799 cm⁻¹ and a low intensity peaks at 962 cm⁻¹ in Raman spectrum. Therefore, these peaks can be rationally attributed to TO phonon scattering peaks of bulk 2H-SiC. The slight shift of SiC frequency in the graph around 1 cm⁻¹ might also be resulted by structural defects presence in the products (Yao et al. 2003; Zou et al. 2006).

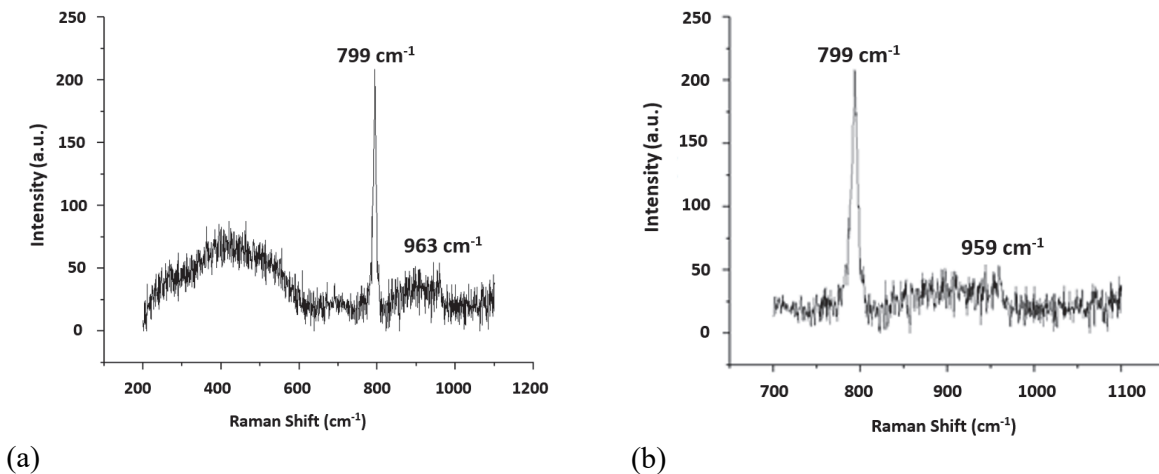


Fig. 4. Raman spectrum of (a) 2H-SiC and (b) 3C-SiC nanowhiskers

The Raman spectroscopy in Fig. 3b shows the pattern of 3C-SiC spectrum. The Raman spectrum is expressed in a form of intensity versus wavenumber (the reciprocal of wavelength, called Raman shift). From the figure, the pattern of the waveforms was similar, but discriminating between them were carried out by looking at the subtle differences in peak positions and intensity ratios. Commonly, the substance 3C-SiC recorded the peaks at 264 cm⁻¹ for transverse acoustic (TA) mode, 764 and 799 cm⁻¹ representing transverse optical (TO) mode and 963 cm⁻¹ resembles longitudinal optical (LO) mode as stated relative to literature (Zhang et al., 2010). This Raman pattern in Raman spectrum indicates a significant peak at 799 cm⁻¹ and a low intensity peaks at 959 cm⁻¹. As a result, these scattering peaks of substance of 3C-SiC can be rationally recognized to TO and LO phonon. There was only 4 cm⁻¹ shift differences between peak positions of SiC frequency which resulted from structural defects existence of the SiC products (Yao et al., 2003; Zou et al., 2006). The shape of a Raman peak is important, not just its position. Whether there is much or little crystallinity can be read from the width of the peak. Any residual stress inside the crystal can also be evaluated from the direction and amount of any shift of the Raman peak. In this experiment, there is no catalyst involved in this reaction, therefore the growth mechanism for this 3C-SiC was proposed to follow vapor-solid (VS) reaction rather than conventional vapor-liquid-solid (VLS) (Moshtaghioun et al., 2011). At 1410 °C melting temperature, the silicon melted and formed a vapor. At that point, silicon in vapor form was conveyed to the carbon atoms by argon gas to form micro-sized SiC

nuclei on the carbon surface. The microcrystal 3C-SiC was changed into nano-structured with increasing reaction time that was fixed to equal for all temperatures, The mechanical treatment done in long milling duration increased the silicon surface contact area. Hence, the elevation of temperature increased the silicon vapor preferring the formation 3C-SiC nanowhiskers. This is covenant with similar finding reported by other researchers (Kang et al., 2011).

4. Conclusions

In summary, the synthesize of nanowhiskers 2H-SiC and 3C-SiC structures by mixture of silicon dioxide and carbon was successfully done using carbothermal reduction process. SEM, XRD and Raman spectroscopy of yield product demonstrated as 2H-SiC with 100 nm in diameters and several microns in length. The slightly shift in 963 cm^{-1} TO phonon Raman frequency indicated staking fault presence in the nanowhiskers structure. The shift differences between peak positions of 3C- SiC frequency in 963 cm^{-1} LO phonon Raman frequency indicated staking faults presence in the nanowhiskers 3C-SiC structure. The formation of both 2H-SiC and 3C-SiC was initiated to be reliant on reaction temperature.

Acknowledgement

The authors want to thank Universiti Teknologi PETRONAS for necessary support throughout the project. This project is financially funded by the Yayasan Universiti Teknologi Petronas under the YUTP-Fundamental Research Grant Scheme (Cost center: 015LCO-247).

References

- Bertilsson, K., Dubaric, E., Nilsson, H. E., Hjelm, M., & Petersson, C. S. (2001). Monte Carlo simulation of vertical MESFETs in 2H, 4H and 6H-SiC. *Diamond and related materials*, 10(3-7), 1283-1286.
- Cetinkaya, S., & Eroglu, S. (2011). Chemical vapor deposition of C on SiO₂ and subsequent carbothermal reduction for the synthesis of nanocrystalline SiC particles/whiskers. *International Journal of Refractory Metals and Hard Materials*, 29(5), 566-572.
- Ganiyu, S. A., Muraza, O., Hakeem, A. S., Alhooshani, K., & Atieh, M. A. (2014). Carbon nanostructures grown on 3D silicon carbide foams: role of intermediate silica layer and metal growth. *Chemical Engineering Journal*, 258, 110-118.
- Heidarzadeh, H., Baghban, H., Rasooli, H., Dolatyari, M., & Rostami, A. (2014). A new proposal for Si tandem solar cell: significant efficiency enhancement in 3C–SiC/Si. *Optik*, 125(3), 1292-1296.
- Ito, A., Kanno, H., & Goto, T. (2015). 2H-SiC films grown by laser chemical vapor deposition. *Journal of the European Ceramic Society*, 35(16), 4611-4615.
- Kang, P., Zhang, B., Wu, G., Su, J., & Gou, H. (2011). Synthesis of SiO₂ covered SiC nanowires with milled Si, C nanopowders. *Materials Letters*, 65(23-24), 3461-3464.
- Kuang, J., Cao, W., & Elder, S. (2013). Synthesis of α-SiC particles at 1200° C by microwave heating. *Powder technology*, 247, 106-111.
- Lee, S. T., Wang, N., & Lee, C. S. (2000). Semiconductor nanowires: synthesis, structure and properties. *Materials Science and Engineering: A*, 286(1), 16-23.
- Li, H., Wu, J., & Wang, Z. M. (Eds.). (2013). *Silicon-based nanomaterials* (Vol. 187). Springer Science & Business Media.
- Morkoc, H., Strite, S., Gao, G. B., Lin, M. E., Sverdlov, B., & Burns, M. (1994). Large-band-gap SiC, III-V nitride, and II-VI ZnSe-based semiconductor device technologies. *Journal of Applied physics*, 76(3), 1363-1398.
- Moshtaghioun, B. M., Monshi, A., Abbasi, M. H., & Karimzadeh, F. (2011). A study on the effects of silica particle size and milling time on synthesis of silicon carbide nanoparticles by carbothermic reduction. *International Journal of Refractory Metals and Hard Materials*, 29(6), 645-650.
- Moskovskikh, D. O., Lin, Y. C., Rogachev, A. S., McGinn, P. J., & Mukasyan, A. S. (2015). Spark plasma sintering of SiC powders produced by different combustion synthesis routes. *Journal of the European Ceramic Society*, 35(2), 477-486.
- Omidí, Z., Ghasemi, A., & Bakhshi, S. R. (2015). Synthesis and characterization of SiC ultrafine particles by means of sol-gel and carbothermal reduction methods. *Ceramics International*, 41(4), 5779-5784.
- Pawelec, A., Strojek, B., Weisbrod, G., & Podsiadło, S. (2002). Preparation of silicon nitride powder from silica and ammonia. *Ceramics international*, 28(5), 495-501.
- Petrovic, J. J., Milewski, J. V., Rohr, D. L., & Gac, F. D. (1985). Tensile mechanical properties of SiC whiskers. *Journal of materials science*, 20(4), 1167-1177.
- Ryu, Z., Zheng, J., Wang, M., & Zhang, B. (2001). Synthesis and characterization of silicon carbide whiskers. *Carbon*, 12(39), 1929-1930.
- Shi, L., Sun, C., Gao, P., Zhou, F., & Liu, W. (2006). Mechanical properties and wear and corrosion resistance of electrodeposited Ni–Co/SiC nanocomposite coating. *Applied Surface Science*, 252(10), 3591-3599.
- Wu, R., Zhou, K., Yue, C. Y., Wei, J., & Pan, Y. (2015). Recent progress in synthesis, properties and potential applications of SiC nanomaterials. *Progress in Materials Science*, 72, 1-60.
- Xu, Y., Zangvil, A., Landon, M., & Thevenot, F. (1992). Microstructure and mechanical properties of hot-pressed silicon carbide-aluminum nitride compositions. *Journal of the American Ceramic Society*, 75(2), 325-333.
- Yao, Y., Lee, S. T., & Li, F. H. (2003). Direct synthesis of 2H–SiC nanowhiskers. *Chemical physics letters*, 381(5-6), 628-633.
- Zhang, H., Ding, W., He, K., & Li, M. (2010). Synthesis and characterization of crystalline silicon carbide nanoribbons. *Nanoscale research letters*, 5(8), 1264-1271.

- Zhu, J., Jia, J., Kwong, F. L., & Ng, D. H. (2013). Synthesis of 6H-SiC nanowires on bamboo leaves by carbothermal method. *Diamond and related materials*, 33, 5-11.
- Zou, G., Dong, C., Xiong, K., Li, H., Jiang, C., & Qian, Y. (2006). Low-temperature solvothermal route to 2H-SiC nanoflakes. *Applied physics letters*, 88(7), 071913.



© 2020 by the authors; licensee Growing Science, Canada. This is an open access article distributed under the terms and conditions of the Creative Commons Attribution (CC-BY) license (<http://creativecommons.org/licenses/by/4.0/>).